# The largest SWI/SNF polyglutamine domain is a pH sensor

J. Ignacio Gutiérrez[1], Greg Brittingham[2], Xuya Wang[2], David Fenyö[2] and Liam J. Holt[2]

1 Department of Molecular and Cell Biology, University of California, Berkeley

2 Institute for Systems Genetics, New York University

## Abstract

**Polyglutamines are known to form aggregates in pathogenic contexts, such as Huntington disease. However, little is known about their normal biological role. We found that the polyglutamine domain of the Snf5 subunit of yeast SWI/SNF complex is required for efficient induction of glucose-repressed genes. Both transient cytosolic acidification and histidines within the polyglutamine domain were required for efficient transcriptional reprogramming. We hypothesized that a pH-dependent oligomerization could be important for *ADH2* expression. In support of this idea, we found that a synthetic spidroin domain from spider silk, which is soluble at pH 7 but oligomerizes at pH ~6.3, could partially complement the function of the *SNF5* polyglutamine domain. These results suggest that the *SNF5* polyglutamine domain is a pH-responsive transcriptional regulator, and provide further evidence of an important biological role for polyglutamine domains beyond the disease context.**

## Introduction

The pH of the cytoplasm and nucleoplasm influences almost all biological processes by determining the protonation state of biological molecules, including the charged amino acid side-chains of proteins, and especially histidines, which have a near-neutral pKa (Whitten, Garcia-Moreno E. and Hilser, 2005). Therefore, pH is tightly regulated in the cell. Early work suggested that nucleocytosoplasmic pH, which we will refer to as $pH_{Cyt}$, from now on, was constant during development (Needham, 1926). However, development of better technologies revealed that $pH_{Cyt}$ does vary and metabolism (Busa and Nuccitelli, 1984; Young *et al.*, 2010), proliferation (Busa and Crowe, 1983) and cell fate (Okamoto, 1994) can be regulated by changes in $pH_{Cyt}$.

The budding yeast *Saccharomyces cerevisiae* is adapted to an acidic environment, and standard growth media is typically at pH 4.0 – 5.5. The plasma membrane proton pump Pma1 and the V-ATPses of the vacuole are the main regulators of cytosolic pH (Martínez-Muñoz and Kane, 2008). Pma1 constantly pumps protons out of the cell to maintain a neutral $pH_{Cyt}$. This process has been estimated to consume up to 20% of cellular ATP (Bracey *et al.*, 1998). When cells are starved for carbon, the Pma1 pump is inactivated, leading to a rapid acidification of the cytosol to pH ~6 (Orij *et al.*, 2009).

Acidification of the cytosol during glucose-starvation is thought to conserve energy, through storage of metabolic enzymes in filamentous aggregates (Petrovska *et al.*, 2014), reduction of macromolecule diffusion (Joyner *et al.*, 2016), decreased membrane biogenesis (Young *et al.*, 2010) and possibly a partial phase transition of the cytoplasm

into a solid-like structure (Joyner *et al.*, 2016; Munder *et al.*, 2016). These studies all highlight inactivation of processes due to decreased $pH_{Cyt}$. However, numerous processes must also be upregulated during carbon starvation to enable adaptation to this stress. In particular, the cell must induce expression of glucose-repressed genes (DeRisi, 1997; Zid and O'Shea, 2014). However, it is still poorly understood how stress gene induction relates to decreased $pH_{Cyt}$.

The Sucrose Non Fermenting genes (SNF) were among the first factors identified for induction of the glucose-repressed genes. Several of these genes were later identified as members of the SWI/SNF complex (Abrams, Neigeborn and Carlson, 1986; Carlson, 1987), an 11 subunit chromatin remodeling enzyme that is highly conserved from yeast to mammals (Peterson and Herskowitz, 1992; Chiba *et al.*, 1994; Peterson, Dingwall and Scott, 1994). The SWI/SNF complex is important for the expression of ~10% of the genes in *Saccharomyces cerevisiae* (~500 genes) (Sudarsanam *et al.*, 2000) during normal vegetative growth, and is also required for efficient transcriptional reprogramming upon carbon starvation. During carbon starvations most genes are down-regulated, but a set of glucose-repressed genes important for adaptation to nutritional stress are strongly induced (Zid and O'Shea, 2014). The SWI/SNF complex is required for the efficient expression of several hundred stress-response and glucose-repressed genes (Sudarsanam *et al.*, 2000; Biddick *et al.*, 2008). Sequence analysis reveals a strong enrichment of low-complexity sequence in the complex. In particular, 4/11 subunits contain polyglutamines (polyQ) or glutamine-rich LCS.

PolyQs have been predominantly studied in the disease context because 9 neurodegenerative illnesses, including Huntington disease, are thought to be caused by toxic aggregation seeded by proteins that contain expanded polyQs (Fan *et al.*, 2014). However, polyQs are relatively abundant in *Eukaryotic* cells: More than 100 human proteins contain polyQs, and the *Dictyostelium* and *Drosophilid* phyla have polyQ structures in ~10% and ~5% of their proteins respectively (Schaefer, Wanker and Andrade-Navarro, 2012). Furthermore, there is clear evidence of purifying selection to maintain polyQs in the *Drosophilids* (Huntley and Clark, 2007). This prevalence and conservation suggests that there must be an important biological function for these repeats. Glutamine rich transactivation domains are an example of functional polyQs, however their precise role in transcriptional activation remains poorly understood (Kadonaga *et al.*, 1987, 1988). Recent work in *Ashbya gosypii* has revealed a role for the phase separation of polyQs in cellular organization (Zhang *et al.*, 2015).

The SWI/SNF complex is a good model system to further investigate the function of polyQ repeats as 4/11 subunits contain polyQ or glutamine-rich LCS, making SWI/SNF the most site of polyQ in the cell. The *SNF5* regulatory subunit contains the largest polyQ of the SWI/SNF complex; this N-terminal LCS domain contains 121 glutamine residues. The polyQ of *SNF5* has been shown to interact with the acidic activator domains of transcription factors GCN4 and VP16 *in vitro* (Prochasson *et al.*, 2003), hinting at a function in recruitment to promoters.

We investigated the relationship between the *SNF5* polyglutamine domain and the cytosolic acidification that occurs during glucose-starvation. By single cell analysis, we found that the dynamics of $pH_{Cyt}$ is highly dynamic and varies between subpopulations of

cells within the same culture. After an initial decrease to $pH_{Cyt}$ <6.5, a subset of cells recovered their $pH_{Cyt}$ to ~7. This transient acidification was required for expression of glucose-repressed genes. The *SNF5* polyglutamine activation domain was also required for timely gene expression, including four histidines that we identify as putative pH sensors. Finally, we propose transient aggregation of low complexity sequences as a possible mechanism for transcriptional reprograming and provide support for this model using an orthogonal pH-dependent aggregation domain.

## Results

### The N-terminal glutamine-rich domain of *SNF5* affects the viability of carbon starved yeast cells in a pH-dependent manner.

First, we compared the fitness of wild-type yeast to strains with a complete deletion of the SNF5 gene (*snf5*Δ), or with a precise deletion of the N-terminal glutamine-rich domain of *SNF5*, referred to as Δ*Q-snf5* (Figure 1A, B). In rich media, the *snf5*Δ strain has a severe growth defect (Figure 1D), while the Δ*Q-snf5* grows at a similar rate to wild-type control cells (Figure 1D). Next, we compared the viability of these strains after an acute switch to synthetic complete medium with no glucose and maintenance in these carbon starvation conditions for 24 hours. Cells were plated before and after starvation and colonies were counted to assess viability. No difference was apparent; all strains maintained 100% viability after starvation (Fig 1C-pH6.5 and below). Therefore, we reasoned that we would need to increase the sensitivity of our assay to reveal a phenotype for our mutants.

Cytosolic acidification is important for viability during carbon starvation: when we buffered the environmental pH ($pH_{Env}$) to 7, thus preventing acidification of the cytosol, wild-type cell viability dropped to 50% (Figure 1C). A strong phenotype was revealed for the Δ*Q-snf5* allele under these conditions: this strain was inviable during starvation at $pH_{Env}$: 7. Furthermore, Δ*Q-snf5* only maintained 25% viability at $pH_{Env}$ 6.75, while the wild-type strain was fully viable. In contrast, the *snf5*Δ strain behaved similarly to wild type in terms of viability during starvation at all $pH_{Env}$ values tested indicating that the null and Δ*Q-snf5* are different. We performed Western blot analysis and observed similar *SNF5* protein levels for all alleles during glucose starvation at both pH 5.0 and 7.5 (Supplemental Figure 8). Thus, the phenotypes that we observed in the Δ*Q-snf5* allele are not due to protein degradation.

SWI/SNF is required for efficient induction of glucose repressed genes when yeast switches to a new carbon source (Sudarsanam *et al.*, 2000; Biddick *et al.*, 2008). We reasoned that the loss of viability in Δ*Q-snf5* strains might be related to a failure to adapt to new carbon sources. To test this idea, we compared the fitness of *SNF5*, *snf5*Δ and Δ*Q-snf5* strains after a switch to galactose, or galactose and ethanol as a carbon source. We observed a long lag-phase and a strong growth defect of the *snf5*Δ strain in these poor carbon sources. In contrast, the Δ*Q-snf5* strain achieved a similar maximal growth rate to control cells, but had an increased lag phase (Supplemental Figure 1A, B). If cells were subjected to glucose starvation for 24 hours prior to the carbon switch we observed

a similar pattern, but the phenotypes were exacerbated (Supplemental Figure 1C, D). These results indicate that *SNF5* is required for the adaptation to new carbon sources and the polyQ of *SNF5* is important for rapid adaptation.

**Induction of the SWI/SNF target *ADH2* in response to carbon starvation requires an acidic environment and the polyQ domain of *SNF5*.**

Alcohol dehydrogenase 2 (*ADH2*) is tightly repressed in the presence of glucose, and is strongly induced upon carbon starvation (Biddick *et al.*, 2008). The SWI/SNF complex is required for the efficient and timely induction of *ADH2* (Young *et al.*, 2008) By RT-Q-PCR, we found that both the N-terminal glutamine rich domain of *SNF5* and an acidic environment are required for transcription of *ADH2* (Figure 2A). After 4 hours of acute carbon starvation at $pH_{Env}$ 6, wild-type cells induce *ADH2* transcription approximately 1000-fold, while Δ*Q-snf5* did not induce detectable levels of transcript. Neither wild-type nor Δ*Q-snf5* strains induced any *ADH2* when the starvation media was adjusted to $pH_{Env}$ 7.4. In contrast the *snf5*Δ strain expressed *ADH2* at slightly lower levels than control in normal starvation, but maintained some expression when the starvation media was adjusted to $pH_{Env}$ 7.4. These results suggest that the *SNF5* subunit is repressive for transcription but somehow acidification of the cytosol during starvation leads to derepression through a mechanism that requires the polyQ domain. Furthermore, we found that Δ*Q-snf5* acts as a dominant-negative allele (Supplemental Figure 7).

To facilitate the further study of the relationship between environmental pH and *ADH2* induction, and to enable the study of gene regulation at a single-cell level, we generated a reporter gene with the mCherry fluorescent protein under the control of the *ADH2* promoter ($P_{ADH2}$-*mCherry*). We then used flow cytometry to quantify levels of red fluorescence. Time course experiments showed that full transcription and translation of the *mCherry* protein took 24 hours, but robust induction was apparent at 6 hours. Induction of $P_{ADH2}$-*mCherry* was clearly bimodal for wild-type cells, indicating substantial cell-to-cell variability in *ADH2* promoter activity under our conditions. This bimodality of *ADH2* induction was lost in the *snf5*Δ null strain, which induced 4-fold less $P_{ADH2}$-*mCherry* than *wild-type*. These data indicate that the polyQ of SNF5 is required for bimodal induction of ADH2. The phenotype of the Δ*Q-snf5* strain was far more severe. This strain completely failed to induce $P_{ADH2}$-*mCherry*. These results are consistent with previous reports where deletion of *SNF5* and *SWI1* polyQs had a more severe phenotype than the double null mutant in some conditions (Prochasson *et al.*, 2003).

We next explored the effect of $pH_{Env}$ on $P_{ADH2}$-*mCherry* expression. Wild-type cells robustly induced $P_{ADH2}$-*mCherry* at all $pH_{Env}$ below 6.5, but almost completely failed to induce the reporter at $pH_{Env}$ of 7.0 and above (Figure 2B, C). In contrast the Δ*Q-snf5* strain failed to induce $P_{ADH2}$-*mCherry* at any $pH_{Env}$. The *snf5*Δ strain showed a decrease of induction efficiency in control conditions ($pH_{Env}$ 5.5) as previously reported (Biddick *et al.*, 2008; Biddick, Law and Young, 2008), however $P_{ADH2}$-*mCherry* induction was much stronger in the deletion strain than in the Δ*Q-snf5* strain. Furthermore, the *snf5*Δ strain still induced some $P_{ADH2}$-*mCherry* at $pH_{Env}$ 7.0, while the wild-type strain failed to induce.

Taken together, these results suggest that *SNF5* is a pH-sensitive regulator of SWI/SNF function that plays both positive and negative regulatory roles. In this model, loss of the polyglutamine domain could lock the SWI/SNF complex in a state that is repressive for glucose repressed genes. We conclude that both the glutamine-rich N-terminus of Snf5 and an acidic environment are required for robust regulation of *ADH2* induction upon carbon starvation.

## Histidines are enriched after poly-glutamine sequences in multiple species

We reasoned that polyQ alone would not be a good pH sensor as glutamine does not change properties over biologically relevant pH ranges. Therefore, to gain further functional insight, we analyzed amino acid enrichments within and around glutamine-rich low complexity sequences. We defined polyQ sequences as a polypeptide sequence containing at least ten glutamines interrupted by no more than two non-glutamine amino acid residues. Within the *S. cerevisiae* proteome, there is a strong enrichment (>3 fold) for histidine and proline within polyQ sequences compared to the global frequency of these amino acids (Figure 3A). For histidine, this enrichment is even more pronounced immediately C-terminal to polyQ repeats (>4 fold). This enrichment of histidines within and immediately after polyQs is also apparent in the human, *Drosophila melanogaster* and *Dictyostelium discoidum* proteomes (Supplemental Figure 2). This enrichment for certain amino acids could be an indication of functional importance, however the codons encoding glutamine (CAG and CAA) are similar to those for histidine (CAT and CAC), therefore random mutations with polyQ-encoding DNA will tend to create histidines with higher probability than other amino acids. Therefore, we tested a null hypothesis that the observed structure of polyQ sequence is due to generation of polyQ repeats (perhaps through CAG repeat expansion) and then mutation of the underlying DNA sequence in the absence of selection. We ran simulations where we allowed CAG, CAA and mixed CAGCAA repeats (artificial polyQ genomes) to randomly mutate at the nucleotide substitution frequencies that have been empirically described for *S. cerevisiae* (Zhu *et al.*, 2014) until the polyQ had degenerated to have around 20% non-Q amino acids (the same frequency as in the true *S. cerevisiae* polyQ structures). The average results of 10,000 simulations are presented as grey bars in figure 3A. While this model does predict enrichment of histidines, the real polyQ structures are significantly more enriched suggesting that there is selective pressure to embed histidine residues within and adjacent to these structures.

## pH changes are sensed by histidines in the N terminal glutamine-rich domain of *Snf5*

The imidazole side chain of histidine has a pKa of around 6, and chemical interactions within the polypeptide can readily shift this value up or down. Therefore, the charge of this amino acid could change as a function of pH changes similar to those reported to

occur in the cytosol of budding yeast under carbon starvation (Orij *et al.*, 2009). The N terminal glutamine-rich domain of Snf5 contains 6 histidines (shown in red and orange in Figure 1B). Therefore, we reasoned that these amino acids might play a pH sensing role. To test this hypothesis, we converted histidines to alanine, the side-chain of which will not change protonation state under any condition. Technical difficulties related to PCR and gene-synthesis within low complexity sequence frustrated attempts to replace all 6 histidines, however, we were able to mutate 4 of 6 histidines to alanine (shown in red in Figure 1B). We refer to this allele as *HtoA-snf5*.

The *HtoA-snf5* allele was almost as severe as a complete deletion of the glutamine rich N-terminal domain. Under optimal pH conditions ($pH_{Env}$ 5.5) both the expression level and fraction of cells that induce is reduced in *HtoA-snf5* strains compared to wild-type (Figure 3B, C). Under less favorable conditions of $pH_{Env}$ 6.5 where WT is still strongly induced, *HtoA-snf5* shows no induction at all. These results indicate that removal of histidines from the *Snf5* N-terminus desensitizes the system to pH change and suggests that these histidines are important for the pH sensing function of *SNF5*.

## Single cell analysis reveals a bimodal pH response to glucose starvation, and that pH recovery precedes *ADH2* expression

Intracellular pH can be studied using pHluorin, a GFP derivative that has been engineered as a ratiometric pH indicator (Miesenböck, De Angelis and Rothman, 1998). Previous studies with pHluorin reported that the cytosolic pH of *S. cerevisiae* drops to around 6 during carbon starvation (Orij *et al.*, 2009). However, these were average population measurements, partly because the original constructs were expressed from a *CEN/ARS* plasmid which leads to cell to cell variability in expression levels. We reengineered pHluorin using the strong *TDH3* promoter and integrated this construct into the *URA3 locus*. Our reengineered pHluorin gave strong expression and was less noisy, enabling single cell pH measurements. We generated strains with both the $P_{ADH2}$-*mCherry* and $P_{TDH3}$-*pHluorin* reporters, allowing us to investigate the dynamics of both pH change and *ADH2* expression.

In wild-type cells, the $pH_{Cyt}$ of the entire population dropped to <6.5 immediately after glucose was removed in starvation media $pH_{Env}$: 5.5. Then, after 30 minutes, the culture began to split into 2 subpopulations: around half of the cells further acidified to $pH_{Cyt}$ 6 and this population failed to induce $P_{ADH2}$-*mCherry*, while the other half recovered their $pH_{Cyt}$ to ~7 and strongly induced $P_{ADH2}$-*mCherry* (Figure 4A, first panel, quantified in Figure 4C, first panel). Wild type cells subjected to acute glucose-starvation at $pH_{Env}$: 7.4, mildly dropped their $pH_{Cyt}$, but not below $pH_{Cyt}$: 6.5 (Figure 4B). Experiments with cycloheximide showed that the initial cytosolic acidification was independent of gene expression, but subsequent neutralization requires protein translation (Supplemental Figure 3).

### *ADH2* induction requires transient acidification of the nucleocytoplasm

The dynamics of $pH_{Cyt}$ and $P_{ADH2}$-*mCherry* suggested that transient acidification could be enough to induce ADH2 expression. We manipulated the environmental pH to test this hypothesis. Wild type cells were subjected to glucose-starvation for 2 hours at $pH_{Env}$ 5 and then the $pH_{Env}$ was alkalinized to 7.4, thus forcing neutralization of the cytosol. pHluorin measurements confirmed that $pH_{cyt}$ of the entire population was forced to 7 by this treatment (Supplemental Figure 4C). Nevertheless, the transient acidification during the first 2 hours of starvation was sufficient to allow robust induction of $P_{ADH2}$-*mCherry* (Supplemental Figure 4B, D). The reverse experiment, where cells are transiently glucose-starved at $pH_{Env}$ 7.4 for 2 h and then switched to $pH_{Env}$ 5 did not lead to efficient induction of $P_{ADH2}$-*mCherry*, despite the $pH_{Cyt}$ drop when switched to $pH_{Env}$ 5 after the 2$^{nd}$ hour (Supplemental Figure 4B, D). We also used sorbic acid, a weak organic acid that can shuttle protons across the plasma membrane (Munder *et al.*, 2016) to prevent $pH_{Cyt}$ recovery during glucose starvation. As expected the entire population remained acidic through the course of the experiment and no $P_{ADH2}$-*mCherry* induction was observed (Supplemental Figure 5). Note, we also used a nuclear localized pHluorin and found that nuclear and cytoplasmic pH values are equivalent in all conditions tested. Together, these results indicate that *ADH2* induction requires a transient drop in $pH_{Cyt}$ at the beginning of glucose-starvation treatment (Supplemental Figure 4) followed by recovery to neutral $pH_{Cyt}$.

### Transient acidification also occurs upon recovery from carbon starvation

To further investigate the role of pH in transcriptional reprograming. We performed single cell analysis of cytoplasmic pH following readdition of glucose to starved cultures. We observed that, indeed there is a rapid, transient $pH_{Cyt}$ drop in the subpopulation of starved cells that had previously induced *ADH2* and recovered their $pH_{Cyt}$ to ~6.8 (Supplemental Figure 6A first panel). All cells then recovered neutral $pH_{Cyt}$ after 30 minutes.

### *SNF5* mutants have an altered pH response upon glucose starvation

We found that *SNF5* plays a role in pH regulation during acute glucose starvation. The *snf5*Δ strain did not acidify as strongly as the wild-type strain, nor did the bifurcation in $pH_{Cyt}$ and *ADH2* expression occur (Figure 4A and C, second panel). In contrast, the Δ*Q*-*snf5* mutant acidified to $pH_{Cyt}$ 6 but then no cells recovered to pH 7 (Figure 4B and C, third panel). The $_{HtoA}$-*snf5* mutant acts as a hypomorph – mostly phenocopying Δ*Q*-*snf5* but a small fraction of cells neutralize and induce *ADH2* at lower levels than wild-type cells (Figure 4B and C, fourth panel).

Together, these results indicate that *SNF5* is involved in pH regulation upon glucose starvation. The C-terminus of the *Snf5* protein is required for proper acidification of the cytosol, while the N-terminal glutamine-rich domain, with histidines intact, is

required for the recovery to neutral pH (probably through transcription of target genes). Thus, *SNF5* appears to both contribute to pH regulation and respond to pH changes through its N-terminal glutamine-rich domain and histidines therein.

## *SNF5* polyQ is required for the efficient induction of a large number of glucose-repressed genes

We performed RNA sequencing analysis to determine the extent of the requirement for the *SNF5* polyQ domains in the activation of glucose-repressed genes. Total RNA was extracted from WT, *ΔQ-snf5* and $_{HtoA}$*-snf5* strains during exponential growth (+Glu) and after 4 hours of glucose starvation.

All three strains showed some degree of upregulation of glucose-repressed genes. However, *ΔQ-snf5* and $_{HtoA}$*-snf5* strains upregulated less genes overall (Figure 5A, B and C). From the >300 genes upregulated upon glucose-starvation in WT, 180 were not upregulated in *ΔQ-snf5* or $_{HtoA}$*-snf5*. Indicating that the majority of genes upregulated during glucose starvation require the polyQ of *SNF5*, and presence of histidine in the *SNF5.* Table 1 lists the 20 most highly induced genes in WT that failed to induce in *ΔQ-snf5* and $_{HtoA}$*-snf5* strains.

Over 300 genes are upregulated in WT strains including *ADH2* and *FBP1*. *ΔQ-snf5* and $_{HtoA}$*-snf5* overlap in most of the genes upregulated, 91 genes are shared among them and only 9 are upregulated in *ΔQ-snf5* and WT but not in $_{HtoA}$*-snf5*, 56 are shared among $_{HtoA}$*-snf5* and WT but not *ΔQ-snf5* (Figure 5D). As expected, many upregulated genes are involved in carbon metabolism or stress response pathways. Indeed, we were able to identify plasma membrane transporters of carbon sources (JEN1, HXT5), several mitochondrial proteins required for metabolism of poor carbon sources (SFC1, ODC1), cytoplasmic metabolism proteins (BAT2, RGI2), members of the transcriptional machinery required for expression of glucose-repressed genes (CAT8, YGR067C) and stress related (HSP26). Table 1 shows the 20 most upregulated genes in WT that are not upregulated in the *ΔQ-snf5* and $_{HtoA}$*-snf5* strains. We also confirmed that mRNA expression levels of our $P_{ADH2}$-mCherry gene are very similar to those of *ADH2*, validating it as a faithful reporter. Therefore, the polyQ of *SNF5* acts as a pH-responsive switch to regulate the expression of a large number of genes.

## Spidroin partially complements the *SNF5* polyQ domain

If the polyQ domain of *SNF5 is a* pH sensor, it may be possible to complement its function with another domain that responds to pH. We also speculated that pH changes might change the oligomerization state of the SWI/SNF complex through the polyQ domain. To test this idea, we took advantage of the spidroin protein. Spidroin, the main component of spider silk, is made and stored in the silk glands of spiders in soluble form at pH ≥7.

The pH of the silk duct decreases from around 7 at the proximal end to ≤6.3 at the distal end causing spidroin to oligomerize into a silk fiber (Askarieh *et al.*, 2011) (Figure 6A). We designed a synthetic mini-spidroin allele of 376 amino acids in length (similar to the size of the polyQ domain). First, we tested if acidification of the cytosol upon glucose starvation could induce aggregation of the spidroin peptide. Exponentially growing cells with a cytosolic pH of 7.4 did not show any spidroin aggregation (data not shown). We then manipulated the cytosolic pH by poisoning glycolysis and the electron transport chain with 10 mM 2-deoxyglucose (2-DG) and 2 nM sodium azide (AZ) respectively. This treatment leads to depletion of ATP causing proton pumps to fails, thereby leading to equilibration of the cytosolic pH with the extracellular pH. Spidroin aggregated in over 90% of cells when the cytosolic pH was reduced to pH 5.5 (Supplemental Figure 9A, B). However, no aggregation was seen in cells treated with 2-DG and AZ at $pH_{Env}$ 7.5 (Supplemental Figure 9A, B). These results indicate that our synthetic mini-spidroin domain changes aggregation state in a pH-dependent manner when expressed in *Saccharomyces cerevisiae*. This aggregation also occurred during carbon starvation: at pH 5.5 around 40% of the cells have clear aggregates while in glucose starvation at pH 7.5 only about 5% do (Supplemental Figure 9B, C).

After confirming that at least 40% of the culture would induce spidroin aggregation upon glucose-starvation at pH 5.5, we fused the mini-spidroin domain to the N-terminus of the *ΔQ-snf5* gene, thus replacing the polyQ of *SNF5* with the spidroin peptide. Amazingly, *Spidroin-ΔQ-snf5* partially rescued the defects observed in the *ΔQ-snf5* strain (Figure 6B, C, D). After a transient acidification ~ 50% of the population induced *ADH2* with mean induction levels reaching 65% of WT control levels (Figure 6C, D). As expected *ADH2* expression was pH sensitive in the *Spidroin-ΔQ-snf5* strain with a $pH_{Env}$ optimum of 5.5, and no induction when $pH_{Env}$ was buffered to 6.5 or above (Figure 6A, B). Thus, *Spidroin-ΔQ-snf5* partially recapitulates the *ADH2* expression and the cytosolic pH dynamics of WT.

We evaluated whether other sequences known to undergo phase transitions, but not affected by pH, could complement *SNF5* polyQ function. We fused the low complexity domains of the FUS and hnRNP proteins to the N-terminus of *ΔQ-snf5*. These domains have been reported to form hydrogels that can recruit RNA-polII (Kato *et al.*, 2012; Kwon *et al.*, 2013). However, these domains couldn't complement polyQ function: *FUS-ΔQ-snf5* and *hnRNP-ΔQ-snf5* both completely failed to induce $P_{ADH2}$-mCherry expression (data not shown). This result suggests that a pH-responsive domain is required for SWI/SNF function.

## Discussion

Dynamic changes in cytosolic pH have been observed in several organisms. pH regulation occurs in many physiological contexts including: cell cycle progression (Gagliardi and Shain, 2013); the circadian rhythm of crassulacean acid metabolism plants (Hafke *et al.*, 2001); oxidative stress (van Schalkwyk *et al.*, 2013); temperature or osmotic shock (Karagiannis and Young, 2001); and changes in nutritional state in *Saccharomyces cerevisiae* (Orij *et al.*, 2009). However, the physiological role of these $pH_{Cyt}$ fluctuations remains poorly understood. Our work establishes a functional link between cytosolic pH changes and gene expression.

Previous studies reported population averages of $pH_{Cyt}$ (Orij *et al.*, 2009) and have emphasized the inactivation of processes in response to cytosolic acidification (Petrovska *et al.*, 2014; Joyner *et al.*, 2016; Munder *et al.*, 2016). However, it is unclear how necessary modifications to the cell can occur if cellular dynamics are uniformly decreased. Much less has been reported regarding a potential positive role of fluctuations in $pH_{cyt}$. Using single cell measurements of both $pH_{Cyt}$ and gene expression we found that two subpopulations arose upon acute glucose-starvation, one with $pH_{Cyt}$ ~5.8 and a second at ~6.2. The latter population recovered neutral $pH_{Cyt}$ and then induced glucose-repressed genes, while the former population remained dormant. We have not yet determined the mechanism that drives the bifurcation in pH response but we could not find any correlation to cell cycle stage or cell age (data not shown). By manipulating the extracellular pH, we found that acidification during the first two hours of glucose-starvation treatment was required for later induction of glucose-repressed genes Thus, transient acidification followed by neutralization may serve as a signal for transcriptional reprogramming while more severe pH decreases may drive alternative cell fates.

In the search for molecular sensors of $pH_{Cyt}$ fluctuations, we found that polyQ sequences are enriched in histidine residues. Histidines are good candidates for pH sensors as they can change protonation state over the recorded range of physiological pH. We focused our studies on the N-terminal region of *SNF5* because it is known to be important for the response to carbon starvation, and contains a large low complexity region enriched in both glutamine and histidine residues. A strain that lacked the polyQ region (*ΔQ-snf5*) still acidified its cytosol upon glucose-starvation. However, it failed to recover to neutral cytosolic pH and was defective in the subsequent expression of ~180 glucose-repressed genes out of the ~300 genes upregulated during glucose-starvation. The histidines within the *SNF5* polyglutamine were also required for transcriptional activation, consistent with their putative pH sensing role. Our high throughput data indicated that *ΔQ-snf5* and $_{HtoA}$*-snf5* largely overlap in their defective transcriptional response upon glucose-starvation. Together, these results suggest that the *SNF5* polyQ domain is a pH sensor and highlight the importance of histidines the sensing mechanism.

PolyQs have been traditionally studied as seeders of aggregation, because toxic polyQ-containing protein aggregation is the molecular basis of 9 neurodegenerative diseases (Fan *et al.*, 2014). The aggregation state of polyQs has been linked to the length

of the homorepeat (Bates *et al.*, 2015; Kuiper *et al.*, 2017). However, recently published evidence indicates that the nature of the residues at the boundaries of polyQs can strongly impact aggregation propensity. For instance, a proline homorepeat at the C-terminal of the Huntingtin protein-polyQ prevents aggregation while 17 residues with an overall positive charge at the N-terminus have the opposite effect, inducing stronger aggregation at neutral pH (Thakur *et al.*, 2015; Shen *et al.*, 2016). Similarly, the addition of two negatively charged residues at the amino end and two positively charged residues at the carboxyl end of the polyQ domain of the yeast Sup35 solubilizes the protein at acidic pH and aggregates at neutral pH while a polyalanine flanked by the same charged amino acid is soluble at all pH values (Perutz *et al.*, 2002). We hypothesize that the protonation state of histidines within or in the boundaries of polyQs regulates their aggregation state. The precise nature of this state remains unclear but could range from an oligomerization to a phase transition similar to those that have been recently described for many other intrinsically disordered domains and proteins (Brangwynne, Mitchison and Hyman, 2011; Kato *et al.*, 2012; Kwon *et al.*, 2013) including polyQ proteins (Zhang *et al.*, 2015). We could not detect large phase separated structures by fluorescence microscopy of Snf5p during glucose-starvation (data not shown). However, it has been recently shown that polyQs made of 34 to 96 glutamines convert between three states: soluble protein, small rapidly-diffusing clusters, large slowly-diffusing aggregates (Li *et al.*, 2016). It is possible that the SWI/SNF complex converts to clusters that are below the diffraction limit of conventional microscopy. Single molecule microscopy (Li *et al.*, 2016) or other super-resolution techniques will be required to directly observe these events, which are likely to be transient in nature and exist only briefly. Nevertheless, we were able to design experiments to address this hypothesis using the spider silk protein, spidroin.

Spidroin is a spider web peptide that is soluble at pH 7 and aggregates at pH 6.3 (Askarieh *et al.*, 2011). Importantly, spidroin does not contain polyglutamine repeats. Thus, spidroin is an orthogonal pH-dependent domain that dynamically changes aggregation states over a similar range of conditions to those sampled during carbon starvation in yeast. This domain allowed us to test our hypothesis that the *SNF5* polyQ undergoes pH-dependent aggregation: If the *ΔQ-snf5* allele is defective due to a failure to aggregate, then adding the synthetic spidroin domain should revert this phenotype. Indeed, we observed that *ADH2* expression was partially recovered in the *spidroin-ΔQ-snf5* strain.

Taken together, our observations are consistent with a two-step model for the induction of glucose repressed genes upon carbon starvation. First, a rapid decrease in $pH_{cyt}$ may disengage most transcription. This inactivation of most genes might involve aggregation of transcriptional regulators including the SWI/SNF complex. Subsequently, some cells undergo a slower recovery of cytoplasmic pH accompanied by expression of glucose-repressed genes. The induction of some of these genes may facilitate pH recovery in a positive feedback. The “aggregated” polyQ could actually be more than one state – for example, solid gel-like and viscous liquid-like behaviors could exist. The fact that acidification followed by neutralization is required for efficient transcriptional

reprogramming suggests that the physical changes in SWI/SNF are transient, but there must be some memory of this event. Several models could account for this memory. For example, transient physical state changes could serve to redistribute the SWI/SNF complex to new loci, change the composition of "super-complexes" of SWI/SNF with other molecules in the nucleus, or recruit enzymes to changes the post-translational modifications on SWI/SNF. Further studies will be required to elucidate the details of the transcriptional reprogramming mechanism.

pH sensing could be a general mechanism for transcriptional reprograming upon environmental changes. We observed that *ΔQ-snf5* has very poor fitness in media supplemented with 1 mM peroxide. Motivated by this result, we tested if there were $pH_{Cyt}$ changes upon oxidative stress. Indeed, cytoplasmic pH dropped rapidly upon peroxide addition and in wild type strains recovered within an hour, while *ΔQ-snf5* cells failed to recover. While the role of SNF5 in oxidative stress remains obscure it is known that the oxidative stress response in baker's yeast requires the *SKN7* transcription factor which interacts with *CYC8* and *TUP1* to activate multiple genes (Brown, Bussey and Stewart, 1994). Interestingly, *SKN7* contains a small polyQ at its C-terminus with multiple embedded histidines, and *CYC8* and *TUP1* also contain polyQs. Therefore, similar pH-dependent aggregation mechanisms may place a role in the oxidative stress response.

During glucose starvation, many SWI/SNF-dependent genes are inactivated and a new set of genes is induced. We speculate that the *SNF5* polyQ domain acts as a "reset" switch to allow this redistribution of the SWI/SNF complex upon starvation. Preliminary biochemical results indicate that SNF5-polyQ undergoes a phase transition into either a viscous liquid droplet or a fiber in a pH- and histidine-dependent manner. We hypothesize that these phase transitions are part of the "reset" mechanism.

All cells must modify gene expression to respond to environmental changes. This phenotypic plasticity is essential to all life, from single celled organisms fighting to thrive in a competitive environment, to the complex genomic reprogramming that must occur during development and tissue homeostasis in the metazoa. Despite the differences between these organisms, the mechanisms that regulate gene expression are highly conserved. This work provides new insights into pH as a signal through which life perceives and reacts to its environment.

**Table 1, top 20 highly expressed genes upon glucose-starvation not upregulated in *ΔQ-snf5* or *HtoA-snf5*.**

| Systematic Name | Standard name | Description |
|---|---|---|
| YLR377C | *FBP1* | Fructose-1,6-bisphosphatase; key regulatory enzyme in the gluconeogenesis pathway, required for glucose metabolism; undergoes either proteasome-mediated or autophagy-mediated degradation depending on growth conditions; glucose starvation results in redistribution to the periplasm; interacts with Vid30p |
| YLR174W | *IDP2* | Cytosolic NADP-specific isocitrate dehydrogenase; catalyzes oxidation of isocitrate to alpha-ketoglutarate; levels are elevated during growth on non-fermentable carbon sources and reduced during growth on glucose; IDP2 has a paralog, IDP3, that arose from the whole genome duplication |
| YKR097W | *PCK1* | Phosphoenolpyruvate carboxykinase; key enzyme in gluconeogenesis, catalyzes early reaction in carbohydrate biosynthesis, glucose represses transcription and accelerates mRNA degradation, regulated by Mcm1p and Cat8p, located in the cytosol |
| YMR303C | ***ADH2*** | Glucose-repressible alcohol dehydrogenase II; catalyzes the conversion of ethanol to acetaldehyde; involved in the production of certain carboxylate esters; regulated by ADR1 |
| YKL217W | *JEN1* | Monocarboxylate/proton symporter of the plasma membrane; transport activity is dependent on the pH gradient across the membrane; mediates high-affinity uptake of carbon sources lactate, pyruvate, and acetate, and also of the micronutrient selenite, whose structure mimics that of monocarboxylates; expression and localization are tightly regulated, with transcription repression, mRNA degradation, and protein endocytosis and degradation all occurring in the presence of glucose |
| YER065C | *ICL1* | Isocitrate lyase; catalyzes the formation of succinate and glyoxylate from isocitrate, a key reaction of the glyoxylate cycle; expression of ICL1 is induced by growth on ethanol and repressed by growth on glucose |
| YJR095W | *SFC1* | Mitochondrial succinate-fumarate transporter; transports succinate into and fumarate out of the mitochondrion; required for ethanol and acetate utilization |
| YJR148W | *BAT2* | Cytosolic branched-chain amino acid (BCAA) aminotransferase; preferentially involved in BCAA catabolism; homolog of murine ECA39; highly expressed during stationary phase and repressed during logarithmic phase; BAT2 has a paralog, BAT1, that arose from the whole genome duplication |
| YIL057C | *RGI2* | Protein of unknown function; involved in energy metabolism under respiratory conditions; expression induced under carbon limitation and repressed under high glucose; RGI2 has a paralog, RGI1, that arose from the whole genome duplication |
| YAR035W | *YAT1* | Outer mitochondrial carnitine acetyltransferase; minor ethanol-inducible enzyme involved in transport of activated acyl groups from the cytoplasm into the mitochondrial matrix; phosphorylated |
| YHR096C | *HXT5* | Hexose transporter with moderate affinity for glucose; induced in the presence of non-fermentable carbon sources, induced by a decrease in growth rate, contains an extended N-terminal domain relative to other HXTs; HXT5 has a paralog, HXT3, that arose from the whole genome duplication |
| YBR072W | *HSP26* | Small heat shock protein (sHSP) with chaperone activity; forms hollow, sphere-shaped oligomers that suppress unfolded proteins aggregation; long-lived protein that is preferentially retained in mother cells and forms |

| | | |
|---|---|---|
| | | cytoplasmic foci; oligomer activation requires heat-induced conformational change; also has mRNA binding activity |
| YBL015W | *ACH1* | Protein with CoA transferase activity; particularly for CoASH transfer from succinyl-CoA to acetate; has minor acetyl-CoA-hydrolase activity; phosphorylated; required for acetate utilization and for diploid pseudohyphal growth |
| YPL134C | *ODC1* | Mitochondrial inner membrane transporter; 2-oxodicarboxylate transporter, exports 2-oxoadipate and 2-oxoglutarate from the mitochondrial matrix to the cytosol for lysine and glutamate biosynthesis and lysine catabolism; suppresses, in multicopy, an fmc1 null mutation; ODC1 has a paralog, ODC2, that arose from the whole genome duplication |
| YDL215C | *GDH2* | NAD(+)-dependent glutamate dehydrogenase; degrades glutamate to ammonia and alpha-ketoglutarate; expression sensitive to nitrogen catabolite repression and intracellular ammonia levels; genetically interacts with GDH3 by suppressing stress-induced apoptosis |
| YNL117W | *MLS1* | Malate synthase, enzyme of the glyoxylate cycle; involved in utilization of non-fermentable carbon sources; expression is subject to carbon catabolite repression; localizes in peroxisomes during growth on oleic acid, otherwise cytosolic; can accept butyryl-CoA as acyl-CoA donor in addition to traditional substrate acetyl-CoA |

## Material and Methods

### Cloning and yeast transformations

Yeast strains used in this study are in the S288c strain-background (derived from BY4743). The sequences of all genes in this study were obtained from the *Saccharomyces cerevisiae* genome database (http://www.yeastgenome.org/).

We cloned the various *SNF5* mutants into plasmids from the Longtine/Pringle collection (Longtine *et al.*, 1998). We assembled plasmids by PCR or gene synthesis (IDT gene-blocks) followed by Gibson cloning (Gibson *et al.*, 2009). Then, plasmids were linearized and used to replace the WT locus by sigma homologous recombination at both ends of the target gene.

The *ΔQ-SNF5* gene lacks the N-terminal 282 amino acids that comprise a glutamine rich low complexity domain. Methionine 283 serves as the ATG for the *ΔQ-SNF5* gene. In the $_{HtoA}$*-SNF5* allele, histidines 106, 109, 213 and 214 were replaced by alanine using mutagenic primers to amplify three fragments of the polyQ region which were combined by Gibson assembly into a *SNF5* parent plasmid linearized with BamH1 and Sac1.

We noticed that the slow growth null strain phenotype of the *snf5Δ* was partially lost over time, presumably due to suppressor mutations. Therefore, to avoid spontaneous suppressors, we first supplemented WT S288c with a CEN/ARS plasmid carrying the *SNF5* gene under its own promoter and the *URA3* auxotrophic selection marker. Then a KanMX resistance cassette, amplified with primers with homology at the 5' and 3' of the *SNF5* gene was used to delete the entire chromosomal *SNF5* ORF by homologous recombination. We cured strains of the CEN/ARS plasmid carrying WT *SNF5* by negative selection against its URA3 locus by streaking for single colonies on 5-FOA plates immediately before each experiment to analyze the ***snf5Δ*** phenotype.

The *ADH2* reporter was cloned into pRS collection plasmids (Chee and Haase, 2012) for integration. *URA3* (pRS306) or *LEU2* (pRS305) were used as auxotrophic selection markers. The 835 base pairs upstream of the +1 of the *ADH2* gene and the mCherry ORF were amplified by PCR and assembled into linearized pRS plasmids (Sac1/Asc1) by Gibson assembly. These plasmids were cut with Sph1 in the middle of the *ADH2* promoter and integrated into the endogenous *ADH2* locus by homologous recombination.

The *pHluorin* gene was clone on a pRS collection plasmid for integration. *URA3* (pRS306) and *LEU2* (pRS305) were used for selection. The plasmid with the *pHluorin* gene was obtained (Orij *et al.*, 2009). We amplified the *pHluorin* gene and the strong TDH3 promoter and used Gibson assembly to clone these fragments into pRS plasmids linearized with Sac1 and Asc1.

A C-terminal TAP tag was used to visualize Snf5 and Snf2 proteins in Western blots. pRS plasmids were used but the cloning strategy was slightly different. A C-terminal region of the *SNF5* and SNF2 genes were PCR amplified without the Stop codon. This segment does not contain a promoter or an ATP codon for translation initiation. The TAP tag was then amplified by PCR and cloned together with the 3' of *SNF5* and *SNF2* by Gibson assembly into pRS plasmids with linearized Sac1 and Asc1. The plasmids linearized in the *snf5* 3' and snf2 3' with StuI and XbaI respectively done to linearize the plasmid allowing integration it into the 3' of each gene locus by homologous recombination. Therefore, after transformation the WT promoter is upstream of the WT gene without the stop codon and fused to the TAP tag.

GFP strains, the *SNF5-GFP* strain was obtained by the yeast GFP collection (Huh *et al.*, 2003), a gift of the Drubin/Barnes laboratory at UC Berkeley. The *SNF2-GFP* fused strain was made by the same approached used for the TAP tagged strain above.

**Culture media**

Most experiments, unless indicated, were performed in synthetic complete media (13.4 g/L yeast nitrogen base and ammonium sulfate; 2 g/L amino acid mix and 2% glucose). Carbon starvation media was synthetic complete without dextrose and supplemented with sorbitol, a non-fermentable carbon source to avoid osmotic shock during glucose-starvation (6.7 g/L YNB + ammonium sulfate; 2g/L Amino acid mix and 100 mM Sorbitol). pH was adjusted using 5 M NaOH.

**Glucose-starvation**

Cultures were incubated in a rotating incubator at 30$^{O}$C and grown overnight (14-16 h) to an OD between 0.2 and 0.3. Note: it is extremely important to prevent culture OD from exceeding 0.3 – and results are different if cells are allowed to saturate and then diluted back. Thus, it is imperative to obtain log phase cultures directly to obtain reproducible results. 3 milliliters of OD 0.2-0.3 culture were centrifuged at 6000 RPM for 3 minutes, re-suspended in SC Sorbitol at different pHs and washed 2 times. Finally, cells were re-suspended in 3 milliliters of SC Sorbitol. For flow cytometry, aliquots of 200 uL were taken for each time point in 96 well plates. During the course of time lapse experiments, culture aliquots were set aside at 4$^{O}$C. LSR II – HTS were used for all measurements. 10,000 cells were measured for each time point.

**Cytosolic pH measurements**

The cytosolic pH measurements were made with flow cytometry or microscopy. *pHluorin* was used to measure pH based on the ratio of fluorescence from two excitation wavelengths. In our cytometry we used the settings for AmCyan (excitation 457, emission 491) and FITC (excitation 494, emission 520). While the AmCyan emission increases with pH, FITC emission decreases. A calibration curve was made in each experiment for each strain. To generate a calibration curve, glycolysis and respiration were poisoned using 2-deoxyglucose and azide leading to equilibration of the cytosolic pH to the extracellular

pH. Although many buffers are available, we used the calibration buffer published by Patricia Kane's group (Diakov, Tarsio and Kane, 2013): 50 mM MES (2-(N-morpholino) ethanesulfonic acid), 50 mM HEPES (4-(2-hydroxyethyl)-1-piperazineethanesulfonic acid, 50 mM KCL, 50 mM NaCL, 0.2 M ammounium acetate, 10 mM sodium azide, 10 mM 2-Deoxyglucose. Buffers were titrated to pH with HCL and NaOH to the desired pH. Sodium Azide and 2-deoxyglucose was always added fresh.

**RT-Q-PCR**

For qPCR and RNA seq, RNA was extracted with the "High pure RNA isolation kit" (Roche) following the manufacturer instructions. Three biological replicates were done for qPCR and RNAseq. cDNAs and qPCR were made with iSCRIPT and iTAQ universal SYBR green supermix by Bio-Rad, following the manufacturer instructions. Samples processed were: Exponentially growing culture (+Glu) and glucose-starvation at pH 5.5 and 7.5 for 4 hours. Primers qPCR were taken from Biddick et al 2008. For *ADH2* and *FBP1* genes are: Forward (GTC TAT CTC CAT TGT CGG CTC)/ Reverse (GCC CTT CTC CAT CTT TTC GTA) and Forward (CTT TCT CGG CTA GGT ATG TTG G)/ Reverse (ACC TCA GTT TTC CGT TGG G). *ACT1* was used as control amplification: Forward (TGG ATT CCG GTG ATG GTG TT)/ Reverse (TCA AAA TGG CGT GAG GTA GAG A).

**RNA sequencing**

We performed RNA sequencing analysis to determine the extent of the requirement for the*SNF5* polyQ domains in the activation of glucose-repressed genes. Total RNA was extracted from WT, *ΔQ-snf5* and $_{HtoA}$*-snf5* strains during exponentially growth (+Glu) and after 4 hours of glucose starvation. Next, Poly-A selection was performed using Dynabeads and libraries were performed following manufactures indications. Sequencing of the 32 samples was performed on an Illumina Hi-seq on two lanes. RNA-seq data were aligned to the University of California, Santa Cruz (UCSC), sacCer2 genome using Kallisto (0.43.0,http://www.nature.com/nbt/journal/v34/n5/full/nbt.3519.html) and downstream visualization and analysis was done using R (3.2.2). Differential gene expression analysis and heat maps were created using Sleuth where a least ratio test was used to determine differentially expressed genes and Euclidean distance to calculate clustering for heat maps.

**Western blot**

Strains containing *SNF5* and *SNF2* fused to the TAP tag were used. Given the low concentration of these proteins, they were extracted with Trichloroacetic acid (TCA): 3 mL or a colony (re-suspended in water) were pelleted by centrifugation for 2 min at 6000 RPM and then frozen in liquid nitrogen. Pellets were thawed on ice and re-suspended in 200 uL of 20% TCA, ~0.4 g of glass beads were added to each tube. Samples were lysed by bead beating 4 times for 2 min with 2 min of resting in ice in each cycle. Supernatants

were extracted using a total of 1 mL of 5% TCA and precipitated for 20 min at 14000 RPM at 4 C. Finally, pellets were re-suspended in 212 uL of Laemmli sample buffer and pH adjusted with ~26 uL of Tris buffer pH 8. Samples were run on 7-12% gradient acrylamide gels with Thermo-Fisher PageRuler Prestained protein ladder 10 to 18 KDa. Once transferred, the membrane was blocked with 5% milk and incubated with a rabbit IgG primary antibody (which is bound by the protein A moiety of the TAP tag) for 1 hour and then with goat anti-rabbit secondary antibody. Membranes were visualized using LiCor Odyssey CLx scanner with Image studio 3.1 software. Membranes were scanned at 700 and 800 nM excitation light.

**Data fitting into Gaussian curves**

The *ADH2* expression inferred from a fluorescent reporter ($P_{ADH2}$-*mCherry)* and cytosolic pH were fitted with a single or double Gaussian curve for statistical analysis, with a Matlab function developed in the lab. The choice of single or double Gaussian fit was determined by assessing which fit gave the least residuals. The height of the single or double Gaussian were used to determine the fraction of cells in each peaks. For simplicity, we quantified the height of the Gaussian rather than the area because peaks overlapped in many conditions.

**Sequence analysis of polyQs**

A polyQ structure in protein sequences was defined as a polypeptide sequence containing at least ten glutamines allowing any number of single or double amino-acid insertions, but broken by any interruption of three or more non-glutamine amino acid residues. For example, QQQQQAAQQQQQ and QAQAQAQAQAQAQAQAQAQ both count as polyQ, but QQQQQAAAQQQQQ does not. *Saccharomyces cerevisiae* genome and protein sequences (S288c) were downloaded from SGD (www.yeastgenome.org). S288c transversion and transition rates were obtained from Zhu *et al*, 2014. We ran a computational evolution experiment with a single nucleotide mutation probability of 0.012 per nucleotide. This simulation leads to a non-synonymous change in roughly 20% of the glutamines, thus maintaining the overall integrity of the polyQ structure but introducing enough changes for statistical analysis. We ran this simulation ten thousand times using the polyQ-encoding portion of the S288c reference genome. Additionally, ten thousand simulations were performed on artificial genomes consisting of pure ‘CAA’, ‘CAG’ or ‘CAGCAA’ until we obtained the same non-glutamine frequency within the polyQ structure as found in S288c protein sequences. We defined an enrichment score as the relative frequency of a specific amino acid residue within or surrounding a polyQ normalized by the overall frequency of this amino acid residue present in the whole reference genome. Besides *Saccharomyces cerevisiae*, enrichment scores within and around polyQ were calculated for *Drosophila melanogaster*, *Homo sapiens* and *Dictyostelium discoideum* reference protein sequences (downloaded from http://www.ebi.ac.uk) (Zhu *et al.*, 2014)

**Table 2: Strains used in this study.**

| |
|---|
| *ura3Δ0 his3Δ0 leu22Δ0 met15Δ0 SNF5* |
| *ura3Δ0 his3Δ0 leu22Δ0 met15Δ0 ΔQ-SNF5::KAN* |
| *ura3Δ0 leu22Δ0 met15Δ0 HtoA-SNF5::HIS3* |
| *ura3Δ0 leu22Δ0 met15Δ0* Spidroin*SNF5::HIS3* |
| *his3Δ0 leu22Δ0 met15Δ0 SNF5 pADH2-mCherry::URA3* |
| *his3Δ0 leu22Δ0 met15Δ0 ΔQ-SNF5::KAN pADH2-mCherry::URA3* |
| *leu22Δ0 met15Δ0 HtoA-SNF5::HIS3 pADH2-mCherry::URA3* |
| *leu22Δ0 met15Δ0* Spidroin*SNF5::HIS3 pADH2-mCherry::URA3* |
| *his3Δ0 met15Δ0 SNF5 pADH2-mCherry::URA3 pHluorin::LEU2* |
| *his3Δ0 met15Δ0 ΔQ-SNF5::KAN pADH2-mCherry::URA3 pHluorin::LEU2* |
| *met15Δ0 HtoA-SNF5::HIS3 pADH2-mCherry::URA3 pHluorin::LEU2* |
| *met15Δ0 SpidroinSNF5::HIS3 pADH2-mCherry::URA3 pHluorin::LEU2* |
| *ura3Δ0 his3Δ0 LEU22Δ0 met15Δ0 SNF5*::KAN *(CEN/ARS-SNF5::URA3)* |
| *ura3Δ0 his3Δ0 met15Δ0 snf5Δ::KAN (CEN/ARS-SNF5::URA3) pADH2-mCherry::LEU2* |
| *ura3Δ0 his3Δ0 met15Δ0 snf5Δ::KAN (CEN/ARS-SNF5::URA3) pADH2-mCherry::LEU2 pHluorin::NAT* |
| *leu22Δ0 met15Δ0 pADH2-mCherry ::URA3 SNF2-TAP::HIS3* |
| *leu22Δ0 met15Δ0 ΔQ-SNF5::HIS3 pADH2-mCherry::URA3 SNF2-TAP::KAN* |
| *leu22Δ0 met15Δ0 HtoA-SNF5::HIS3 pADH2-mCherry::URA3 SNF2-TAP::KAN* |
| *his3Δ0 met15Δ0 (CEN/ARS-SNF5::URA) SNF5::KAN pADH2-mCherry::LEU2 SNF2-TAP::NATMX* |
| *his3Δ0 met15Δ0 SNF5::KAN pADH2-mCherry::LEU2 (CEN/ARS-SNF5::URA3)* |
| *his3Δ0 met15Δ0 ΔQ-SNF5::KAN pADH2-mCherry::LEU2 (CEN/ARS-SNF5::URA3)* |

## References

Abrams, E., Neigeborn, L. and Carlson, M. (1986) 'Molecular analysis of SNF2 and SNF5, genes required for expression of glucose-repressible genes in Saccharomyces cerevisiae.', *Molecular and cellular biology*, 6(11), pp. 3643–51. doi: 10.1128/mcb.6.11.3643.

Askarieh, G., Hedhammar, M., Nordling, K., Saenz, A., Casals, C., Rising, A., Johansson, J. and Knight, S. D. (2011) 'Self-assembly of spider silk proteins is controlled by a pH-sensitive relay', *Nature*. Nature Publishing Group, 465(7295), pp. 236–238. doi: 10.1038/nature08962.

Bates, G. P., Dorsey, R., Gusella, J. F., Hayden, M. R., Kay, C., Leavitt, B. R., Nance, M., Ross, C. A., Scahill, R. I., Wetzel, R., Wild, E. J. and Tabrizi, S. J. (2015) 'Huntington disease', *Nature Reviews Disease Primers*, (April), p. 15005. doi: 10.1038/nrdp.2015.5.

Biddick, R. K., Law, G. L., Chin, K. K. B. and Young, E. T. (2008) 'The transcriptional coactivators SAGA, SWI/SNF, and mediator make distinct contributions to activation of glucose-repressed genes', *Journal of Biological Chemistry*, 283(48), pp. 33101–33109. doi: 10.1074/jbc.M805258200.

Biddick, R. K., Law, G. L. and Young, E. T. (2008) 'Adr1 and Cat8 mediate coactivator recruitment and chromatin remodeling at glucose-regulated genes', *PLoS ONE*, 3(1). doi: 10.1371/journal.pone.0001436.

Bracey, D., Holyoak, C. D., Nebe-Von Caron, G. and Coote, P. J. (1998) 'Determination of the intracellular pH (pH(i)) of growing cells of Saccharomyces cerevisiae: The effect of reduced-expression of the membrane H+-ATPase', *Journal of Microbiological Methods*, 31(3), pp. 113–125. doi: 10.1016/S0167-7012(97)00095-X.

Brangwynne, C. P., Mitchison, T. J. and Hyman, A. A. (2011) 'Active liquid-like behavior of nucleoli determines their size and shape in Xenopus laevis oocytes', *Proc. Natl. Acad. Sci.*, 108(11), pp. 4334–4339. doi: 10.1073/pnas.1017150108.

Brown, J. L., Bussey, H. and Stewart, R. C. (1994) 'Yeast Skn7p functions in a eukaryotic two-component regulatory pathway.', *The EMBO journal*, 13(21), pp. 5186–94.

Busa, W. B. and Crowe, J. H. (1983) 'Intracellular pH Regulates Transitions between Dormancy and Development of Brine Shrimp (Artemia salina) Embryos', *Science*, 221(4608), pp. 366–368. doi: 10.1126/science.221.4608.366.

Busa, W. B. and Nuccitelli, R. C. N.-C. (1984) 'Metabolic regulation via intracellular pH', *Am J Physiol Regul Integr Comp Physiol*, 246, pp. R409–R438.

Carlson, M. (1987) 'Regulation of sugar utilization in Saccharomyces species.', *Journal of Bacteriology*, 169(11), pp. 4873–4877.

Chee, M. K. and Haase, S. B. (2012) 'New and Redesigned pRS Plasmid Shuttle Vectors for Genetic Manipulation of *Saccharomyces cerevisiae*', *G3: Genes|Genomes|Genetics*, 2(5), pp. 515–526. doi: 10.1534/g3.111.001917.

Chiba, H., Muramatsu, M., Nomoto, A. and Kato, H. (1994) 'Two human homologues of saccharomyces cerevisiae SWI2/SNF2 and Drosophila brahma are transcriptional coactivators cooperating with the estrogen receptor and the retinoic acid receptor', *Nucleic Acids Research*, 22(10), pp. 1815–1820. doi: 10.1093/nar/22.10.1815.

DeRisi, J. L. (1997) 'Exploring the Metabolic and Genetic Control of Gene Expression on a Genomic Scale', *Science*, 278(5338), pp. 680–686. doi: 10.1126/science.278.5338.680.

Diakov, T. T., Tarsio, M. and Kane, P. M. (2013) 'Measurement of vacuolar and cytosolic pH in vivo in yeast cell suspensions.', *Journal of visualized experiments : JoVE*, (74), pp. 1–7. doi: 10.3791/50261.

Fan, H., Ho, L., Chi, C., Chen, S., Peng, G., Chan, T., Lin, S. and Harn, H. (2014) 'Review Polyglutamine ( PolyQ ) Diseases : Genetics to Treatments', 23(235), pp. 441–458. doi: 10.3727/096368914X678454.

Gagliardi, L. J. and Shain, D. H. (2013) 'Is intracellular pH a clock for mitosis?', *Theoretical biology & medical modelling*, 10(1), p. 8. doi: 10.1186/1742-4682-10-8.

Gibson, D. G., Young, L., Chuang, R.-Y., Venter, J. C., Hutchison, C. a, Smith, H. O., Iii, C. A. H. and America, N. (2009) 'Enzymatic assembly of DNA molecules up to several hundred kilobases.', *Nature methods*, 6(5), pp. 343–5. doi: 10.1038/nmeth.1318.

Hafke, J. B., Neff, R., Hütt, M. T., Lüttge, U. and Thiel, G. (2001) 'Day-to-night variations of cytoplasmic pH in a crassulacean acid metabolism plant.', *Protoplasma*, 216(3–4), pp. 164–70.

Huh, W.-K., Falvo, J. V., Gerke, L. C., Carroll, A. S., Howson, R. W., Weissman, J. S. and O'Shea, E. K. (2003) 'Global analysis of protein localization in budding yeast', *Nature*, 425(6959), pp. 686–691. doi: 10.1038/nature02026.

Huntley, M. A. and Clark, A. G. (2007) 'Evolutionary analysis of amino acid repeats across the genomes of 12 drosophila species', *Molecular Biology and Evolution*, 24(12), pp. 2598–2609. doi: 10.1093/molbev/msm129.

Joyner, R. P., Tang, J. H., Helenius, J., Dultz, E., Brune, C., Holt, L. J., Huet, S., M??ller, D. J. and Weis, K. (2016) 'A glucose-starvation response regulates the diffusion of macromolecules', *eLife*, 5(MARCH2016), pp. 1–26. doi: 10.7554/eLife.09376.

Kadonaga, J. T., Carner, K. R., Masiarz, F. R. and Tjian, R. (1987) 'Isolation of cDNA encoding transcription factor Sp1 and functional analysis of the DNA binding domain.', *Cell*, 51(6), pp. 1079–1090. doi: 0092-8674(87)90594-0 [pii].

Kadonaga, J. T., Courey, A. J., Ladika, J. and Tjian, R. (1988) 'Distinct regions of Sp1 modulate DNA binding and transcriptional activation', *Science*, 242(4885), pp. 1566–1570.

Karagiannis, J. and Young, P. G. (2001) 'Intracellular pH homeostasis during cell-cycle progression and growth state transition in Schizosaccharomyces pombe.', *Journal of cell science*, 114(Pt 16), pp. 2929–41. doi: 10.1091/mbc.E04.

Kato, M., Han, T. W., Xie, S., Shi, K., Du, X., Wu, L. C., Mirzaei, H., Goldsmith, E. J., Longgood, J., Pei, J., Grishin, N. V., Frantz, D. E., Schneider, J. W., Chen, S., Li, L., Sawaya, M. R., Eisenberg, D., Tycko, R. and McKnight, S. L. (2012) 'Cell-free Formation of RNA Granules: Low Complexity Sequence Domains Form Dynamic Fibers within Hydrogels', *Cell*, 149(4), pp. 753–767. doi: 10.1016/j.cell.2012.04.017.

Kuiper, E. F. E., de Mattos, E. P., Jardim, L. B., Kampinga, H. H. and Bergink, S. (2017) 'Chaperones in Polyglutamine Aggregation: Beyond the Q-Stretch', *Frontiers in Neuroscience*, 11(March), pp. 1–11. doi: 10.3389/fnins.2017.00145.

Kwon, I., Kato, M., Xiang, S., Wu, L., Theodoropoulos, P., Mirzaei, H., Han, T., Xie, S., Corden, J. L. and McKnight, S. L. (2013) 'Phosphorylation-Regulated Binding of RNA Polymerase II to Fibrous Polymers of Low-Complexity Domains', *Cell*. Elsevier, 155(5), pp. 1049–1060. doi: 10.1016/j.cell.2013.10.033.

Li, L., Liu, H., Dong, P., Li, D., Legant, W. R., Grimm, J. B., Lavis, L. D., Betzig, E., Tjian, R. and Liu, Z. (2016) 'Real-time imaging of Huntingtin aggregates diverting target search and gene transcription', *eLife*, 5(AUGUST), pp. 1–29. doi: 10.7554/eLife.17056.001.

Longtine, M. S., McKenzie, A., Demarini, D. J., Shah, N. G., Wach, A., Brachat, A., Philippsen, P. and Pringle, J. R. (1998) 'Additional modules for versatile and economical PCR-based gene deletion and modification in Saccharomyces cerevisiae', *Yeast*, 14(10), pp. 953–961. doi: 10.1002/(SICI)1097-0061(199807)14:10<953::AID-YEA293>3.0.CO;2-U.

Martínez-Muñoz, G. A. and Kane, P. (2008) 'Vacuolar and plasma membrane proton pumps collaborate to achieve cytosolic pH homeostasis in yeast', *Journal of Biological Chemistry*, 283(29), pp. 20309–20319. doi: 10.1074/jbc.M710470200.

Miesenböck, G., De Angelis, D. a and Rothman, J. E. (1998) 'Visualizing secretion and synaptic transmission with pH-sensitive green fluorescent proteins.', *Nature*, 394(6689), pp. 192–5. doi: 10.1038/28190.

Munder, M. C., Midtvedt, D., Franzmann, T., Nüske, E., Otto, O., Herbig, M., Ulbricht, E., Müller, P., Taubenberger, A., Maharana, S., Malinovska, L., Richter, D., Guck, J., Zaburdaev, V. and Alberti, S. (2016) 'A pH-driven transition of the cytoplasm from a fluid- to a solid-like state promotes entry into dormancy', *eLife*. eLife Sciences Publications Limited, 5, pp. 59–69. doi: 10.7554/eLife.09347.

Needham, J. (1926) 'The Hydrogen-Ion Concentration and Oxidation-Reduction Potential of the Cell-Interior before and after Fertilisation and Cleavage : A Micro-Injection Study on Marine Eggs Author ( s ): Joseph Needham and Dorothy Moyle Needham Source : Proceedings of the R', 99(695), pp. 173–199.

Okamoto, Y. K. K. (1994) 'Cytoplasmic Ca+2 and H+ concentrations determine cell fate in Dictyostelium discoideum', *Access*, 28(13), pp. 2423–2427.

Orij, R., Postmus, J., Beek, A. Ter, Brul, S. and Smits, G. J. (2009) 'In vivo measurement of cytosolic and mitochondrial pH using a pH-sensitive GFP derivative in Saccharomyces cerevisiae reveals a relation between intracellular pH and growth', *Microbiology*, 155(1), pp. 268–278. doi: 10.1099/mic.0.022038-0.

Perutz, M. F., Pope, B. J., Owen, D., Wanker, E. E. and Scherzinger, E. (2002) 'Aggregation of proteins with expanded glutamine and alanine repeats of the glutamine-rich and asparagine-rich domains of Sup35 and of the amyloid β-peptide of amyloid plaques', *Proceedings of the National Academy of Sciences of the United States of America*, 99(8), pp. 5596–5600. doi: 10.1073/pnas.042681599.

Peterson, C. L., Dingwall, A. and Scott, M. P. (1994) 'Five SWI/SNF gene products are components of a large multisubunit complex required for transcriptional enhancement.', *Proceedings of the National Academy of Sciences of the United States of America*, 91(8), pp. 2905–8.

Peterson, C. L. and Herskowitz, I. (1992) 'Characterization of the yeast SWI1, SWI2, and SWI3 genes, which encode a global activator of transcription', *Cell*, 68(3), pp. 573–583. doi: 10.1016/0092-8674(92)90192-F.

Petrovska, I., Nüske, E., Munder, M. C., Kulasegaran, G., Malinovska, L., Kroschwald, S., Richter, D., Fahmy, K., Gibson, K., Verbavatz, J. M. and Alberti, S. (2014) 'Filament formation by metabolic enzymes is a specific adaptation to an advanced state of cellular starvation', *eLife*, 2014(3), pp. 1–19. doi: 10.7554/eLife.02409.

Prochasson, P., Neely, K. E., Hassan, A. H., Li, B. and Workman, J. L. (2003) 'Targeting activity is required for SWI/SNF function in vivo and is accomplished through two partially redundant activator-interaction domains', *Molecular Cell*, 12(4), pp. 983–990. doi: 10.1016/S1097-2765(03)00366-6.

Schaefer, M. H., Wanker, E. E. and Andrade-Navarro, M. A. (2012) 'Evolution and function of CAG/polyglutamine repeats in protein-protein interaction networks', *Nucleic Acids Research*, 40(10), pp. 4273–4287. doi: 10.1093/nar/gks011.

van Schalkwyk, D. A., Saliba, K. J., Biagini, G. A., Bray, P. G. and Kirk, K. (2013) 'Loss of pH Control in Plasmodium falciparum Parasites Subjected to Oxidative Stress', *PLoS ONE*, 8(3). doi: 10.1371/journal.pone.0058933.

Shen, K., Calamini, B., Fauerbach, J. A., Ma, B., Shahmoradian, S. H., Serrano Lachapel, I. L., Chiu, W., Lo, D. C. and Frydman, J. (2016) 'Control of the structural

landscape and neuronal proteotoxicity of mutant Huntingtin by domains flanking the polyQ tract.', *eLife*, 5, pp. 1–29. doi: 10.7554/eLife.18065.

Sudarsanam, P., Iyer, V. R., Brown, P. O. and Winston, F. (2000) 'Whole-genome expression analysis of snf/swi mutants of Saccharomyces cerevisiae.', *Proceedings of the National Academy of Sciences of the United States of America*, 97(7), pp. 3364–3369. doi: 10.1073/pnas.97.7.3364.

Thakur, A. K., Jayaraman, M., Mishra, R., Thakur, M., Chellgren, V. M., Byeon, I.-J. L., Anjum, D. H., Kodali, R., Creamer, T. P., Conway, J. F., Gronenborn, A. M. and Wetzel, R. (2015) 'Polyglutamine disruption of the huntingtin exon 1 N terminus triggers a complex aggregation mechanism'. doi: 10.1038/nsmb.1570.

Whitten, S. T., Garcia-Moreno E., B. and Hilser, V. J. (2005) 'Local conformational fluctuations can modulate the coupling between proton binding and global structural transitions in proteins', *Proceedings of the National Academy of Sciences*, 102(12), pp. 4282–4287. doi: 10.1073/pnas.0407499102.

Young, B. P., Shin, J. J. H., Orij, R., Chao, J. T., Li, S. C., Guan, X. L., Khong, A., Jan, E., Wenk, M. R., Prinz, W. A., Smits, G. J. and Loewen, C. J. R. (2010) 'Phosphatidic Acid Is a pH Biosensor That Links Membrane Biogenesis to Metabolism', *Science*, 329(5995), pp. 1085–1088. doi: 10.1126/science.1191026.

Young, E. T., Tachibana, C., Chang, H.-W. E., Dombek, K. M., Arms, E. M. and Biddick, R. (2008) 'Artificial recruitment of mediator by the DNA-binding domain of Adr1 overcomes glucose repression of ADH2 expression', *Molecular and cellular biology*, 28(8), pp. 2509–2516. doi: 10.1128/MCB.00658-07.

Zhang, H., Elbaum-Garfinkle, S., Langdon, E. M., Taylor, N., Occhipinti, P., Bridges, A. A., Brangwynne, C. P. and Gladfelter, A. S. (2015) 'RNA Controls PolyQ Protein Phase Transitions', *Molecular Cell*. Elsevier Inc., 60(2), pp. 220–230. doi: 10.1016/j.molcel.2015.09.017.

Zhu, Y. O., Siegal, M. L., Hall, D. W. and Petrov, D. A. (2014) 'Precise estimates of mutation rate and spectrum in yeast.', *Proceedings of the National Academy of Sciences of the United States of America*, 111(22), pp. E2310-8. doi: 10.1073/pnas.1323011111.

Zid, B. M. and O'Shea, E. K. (2014) 'Promoter sequences direct cytoplasmic localization and translation of mRNAs during starvation in yeast. TL - 514', *Nature*. Nature Publishing Group, 514 VN-(7520), pp. 117–121. doi: 10.1038/nature13578.

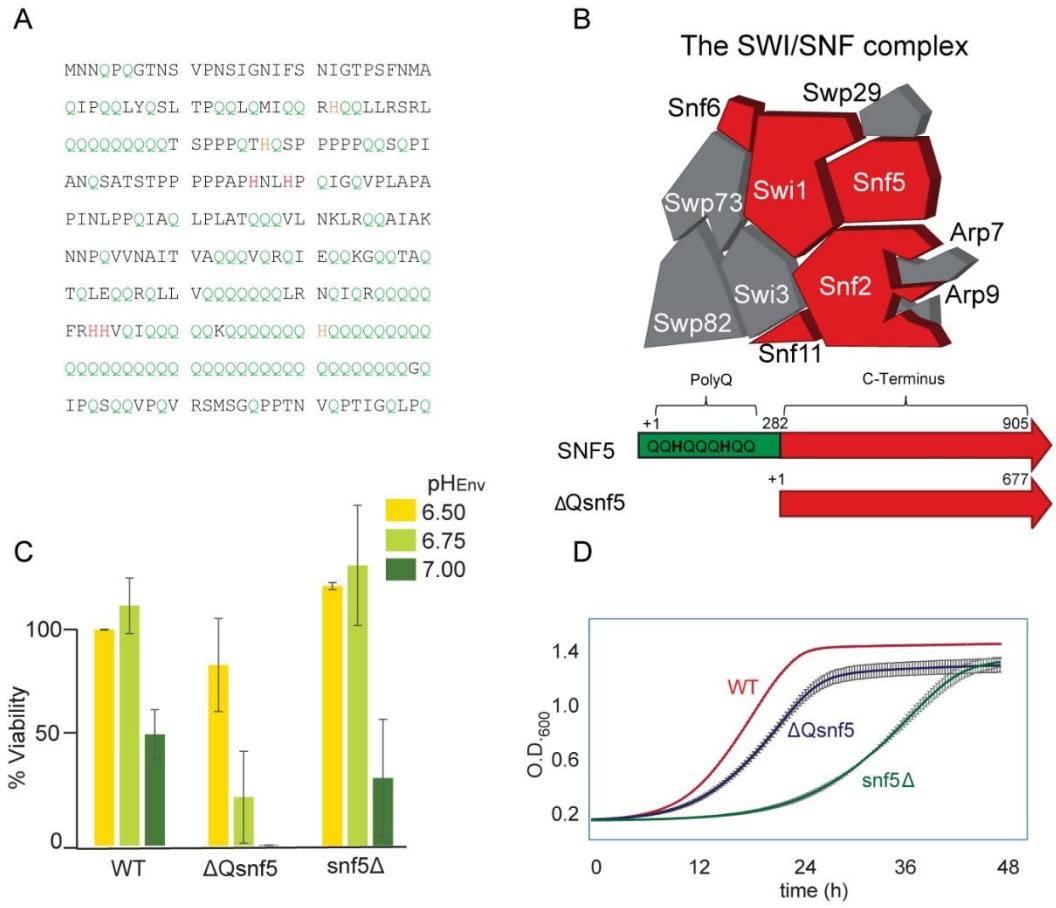


**Figure 1: Deletion of the *Snf5* polyglutamine leads to loss of viability in carbon starvation, especially at neutral environmental pH.** A- The 288 amino acids of the polyQ domain of *SNF5*, glutamine is shown in green and histidine in red/orange. B- Schematic representation of the SWI/SNF according to the available structural data, in red are the subunits that contain polyQ sequences, in the bottom of B is a schematic representation of the *SNF5* gene with its polyQ domain indicated at the N-terminus (Green). C -Viability after 24 h of glucose-starvation at $pH_{Env}$ 6.5 (Yellow), 6.75 (Light Green) and 7.0 (Dark Green). D- Growth curves for WT, *ΔQ-snf5* and *snf5Δ* strains.

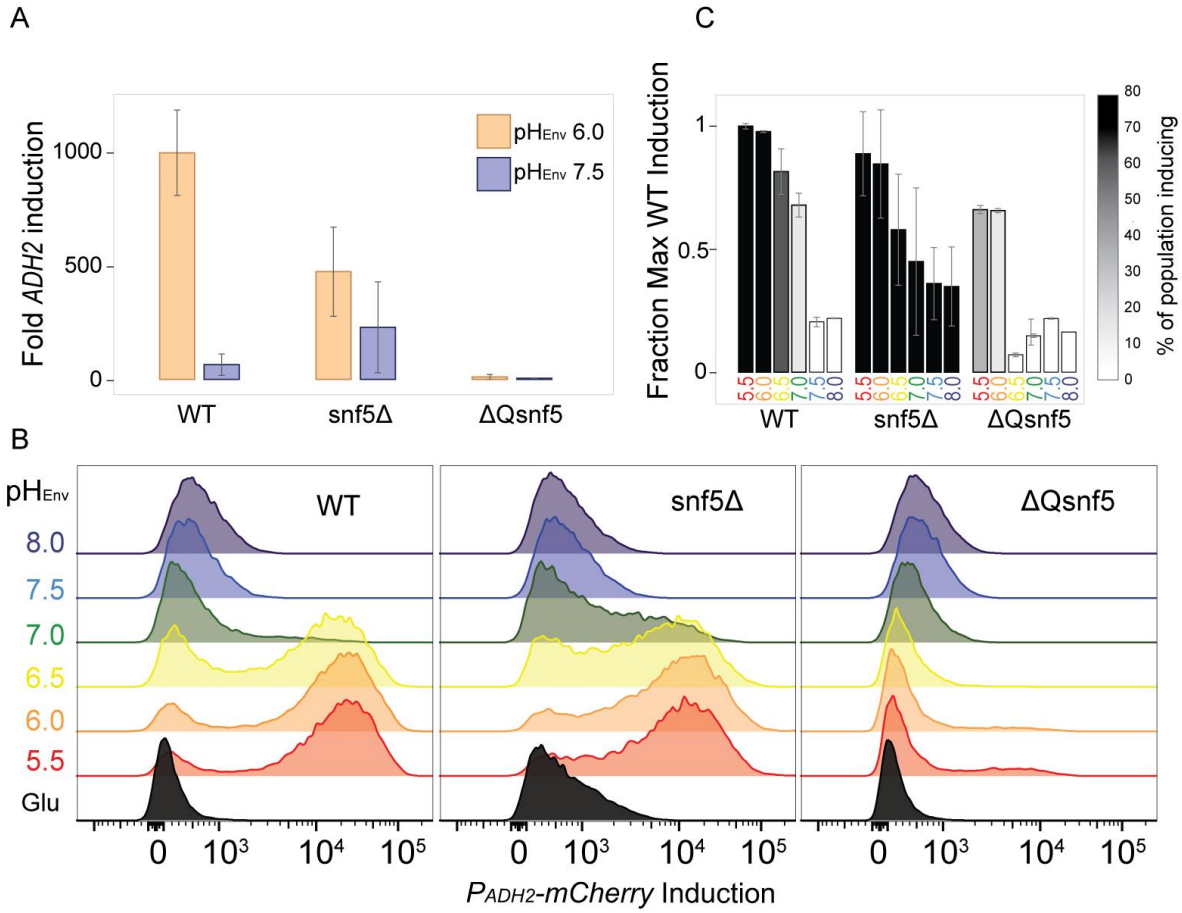


**Figure 2: *ADH2* expression requires an acidic environmental pH and the *SNF5* polyglutamine.** A- RT-QPCR experiments to determine *ADH2* mRNA content of each strain after 4 h of glucose-starvation at $pH_{Env}$ 6.0 (orange) and $pH_{Env}$ 7.5 (blue). *ACT1* mRNA was used as a control, Y axis corresponds to fold induction of *ADH2* mRNA on glucose-starvation over exponentially growing cells. B- Cytometry data histograms of $P_{ADH2}$-*mCherry* induction. Environmental pH is indicated by color codes in B and C: pH 5.5 (red), pH 6.0 (orange), pH 6.5 (yellow), pH 7.0 (green), pH 7.5 (blue) and pH 8.0 (purple). C- Expression of $P_{ADH2}$-*mCherry* fluorescent reporter integrated at the *ADH2* locus, upon starvation at different pH. Raw data was quantified by fitting to single or double Gaussian models (see material and methods) to quantify relative levels of gene induction (bar height) and the fraction of cells inducing (bar shade).

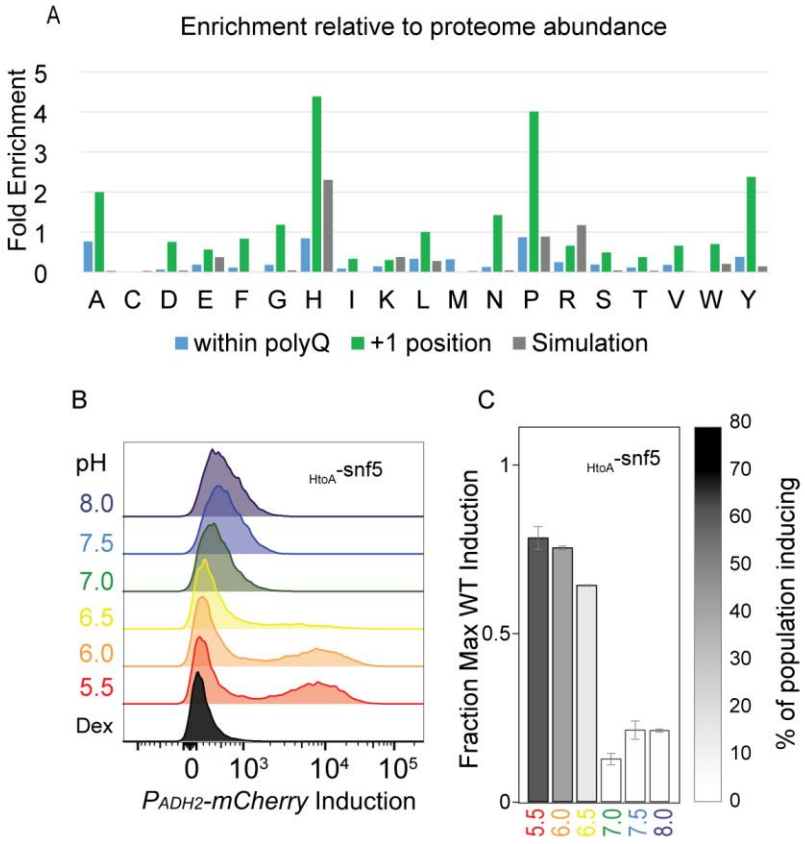


**Figure 3: Histidines are important for the function of the *SNF5* polyglutamine domain.** A- Sequence analysis results for all *Saccharomyces cerevisiae* polyQs, showing frequencies of each amino acid compared to the proteome average, within polyQ structures (blue), and immediately C-terminal to the structures (the +1 position, green). We also show expected frequencies generated for a null-hypothesis where all sequences are generated from a pure polyQ, followed by neutral evolution – results are averages of 10,000 simulations (grey). B- Cytometry data showing levels of induction of $P_{ADH2}$-*mCherry* after 6 h glucose-starvation in a strain harboring an allele of *SNF5* in which 4 of 6 histidines in the polyglutamine are mutated to alanine (*HtoA-snf5*). C- Data from B was quantified by fitting to a single or double Gaussian model Expression levels are relative to wild type expression.

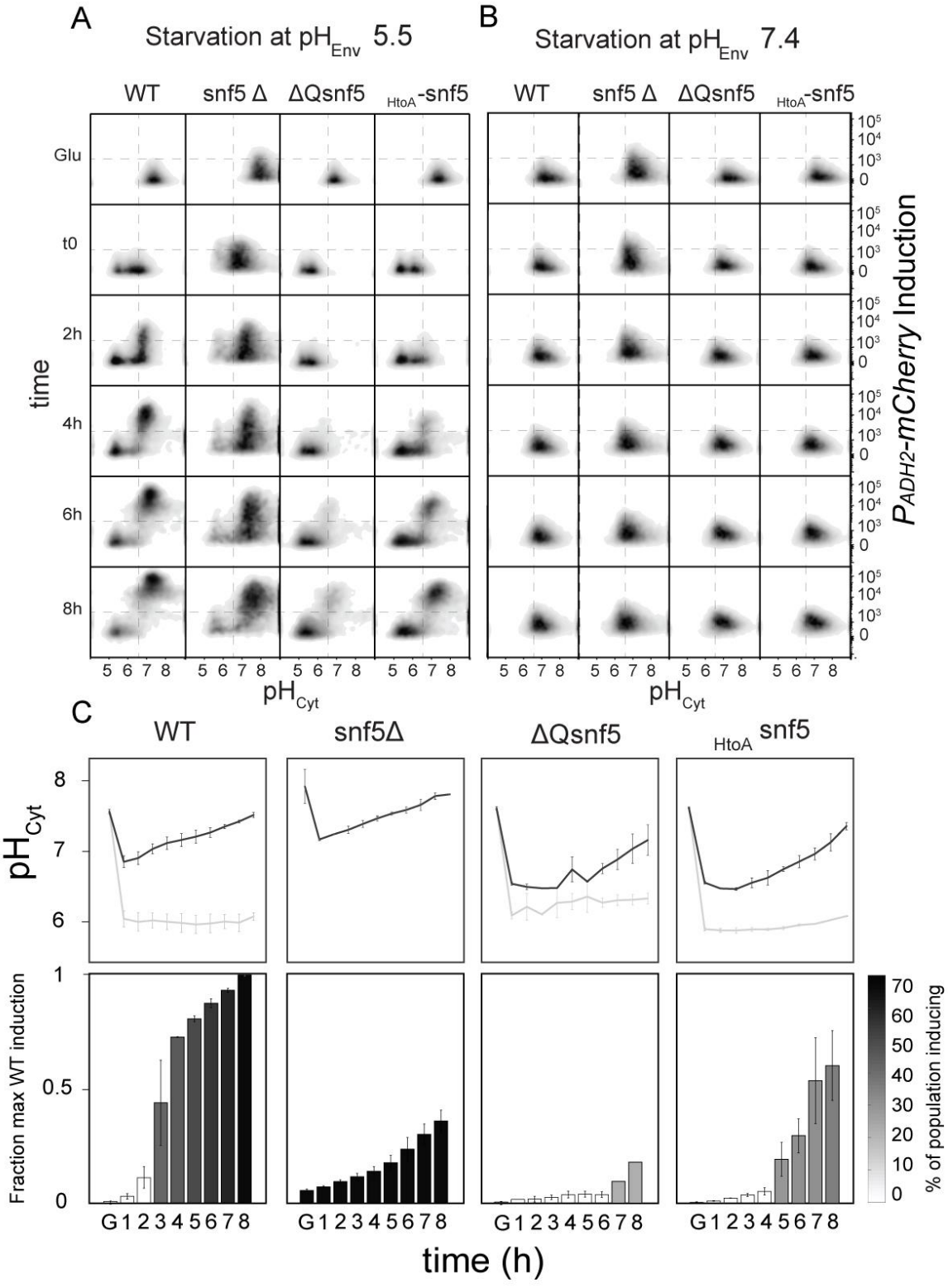

**Figure 4: Single cell analysis reveals a bifurcation in behavior upon glucose-starvation: One subpopulation acidifies to pH 6 and fails to induce, while a second subpopulation transiently acidifies and then induces *ADH2.*** A- Dot plots of cytometry data quantifying cytosolic pH (x-axis) and induction of $P_{ADH2}$-*mCherry* (y-axis) in glucose-starvation media at $pH_{Env}$: 5.5. Columns show WT, *snf5Δ, ΔQ-snf5* and $_{HtoA}$-*snf5* strains (left to right). Rows are time points starting from with logarithmically growing cells prior to dextrose wash out "Glu". 10,000 cells were sampled at each time point. B-Same than A, but on glucose-starvation media $pH_{Env}$: 7.5. C- Raw data from A was fitted to single or double Gaussian models (see materials and methods). Top panels show quantification of cytosolic pH, each time point has one or two peaks and where there are two lines (black and grey), these represent the median pH values for the more neutral and more acidic populations respectively. Bottom panels show levels of induction of the $P_{ADH2}$-*mCherry* expression. Bar height indicates to the intensity of mCherry fluorescence (normalized to maximum values for the WT control strain) and the color code represents the percentage of the population that induces the $P_{ADH2}$-*mCherry* reporter above background levels.

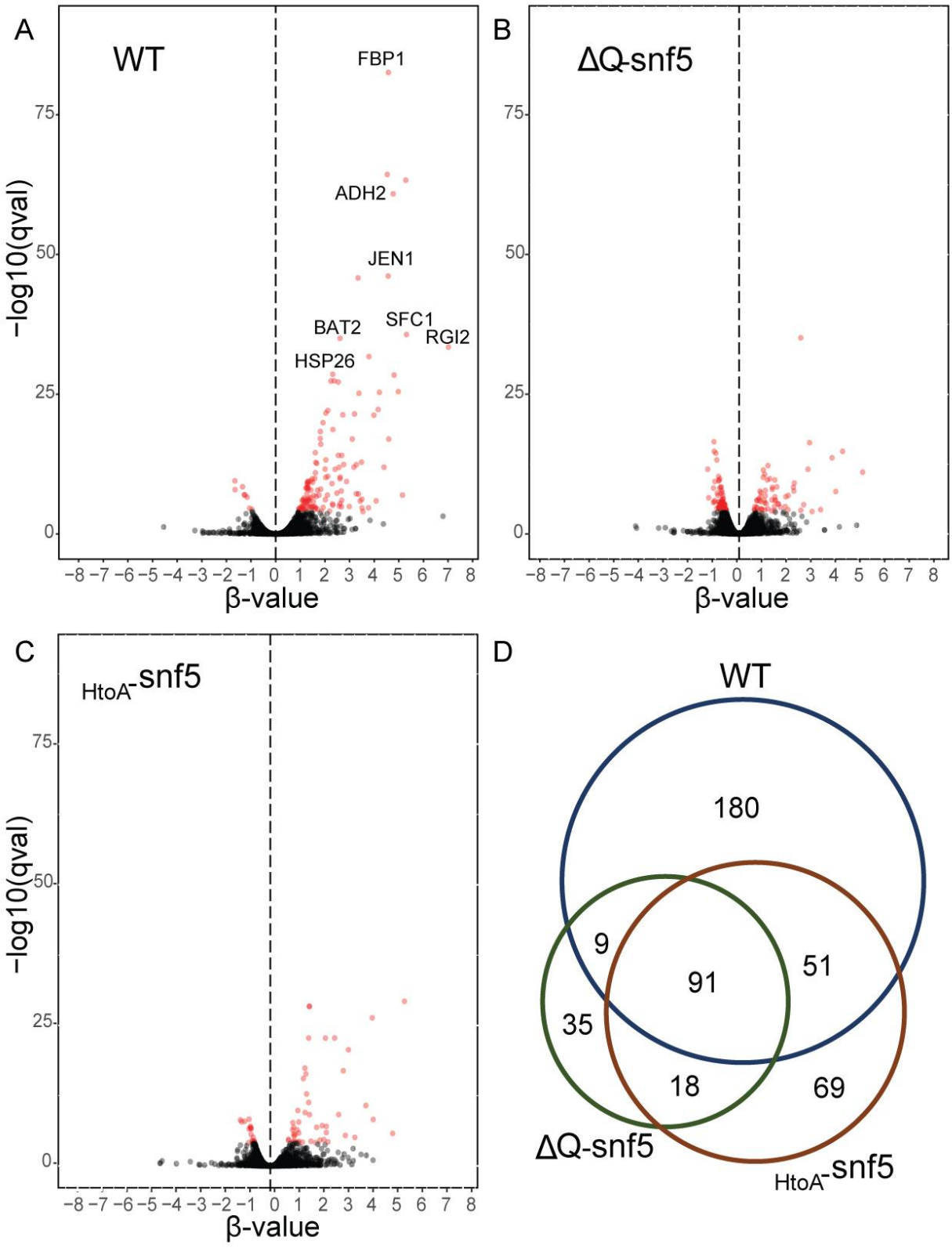

**Figure 5: RNA-seq analysis reveals widespread polyQ-dependence in the expression of glucose repressed genes.** A- Volcano plot of WT in “Glu” vs carbon starvation: x-axis is the natural logarithm of the ratio of expression in dextrose versus carbon starvation with repressed genes to the left of the origin and induced genes to the right, y-axis is the p-value for difference (negative $\log_{10}$ scale). Red dots indicate genes expressed to significantly different levels. Black dots are non-significantly different. B and C show the same volcano plots for *ΔQ-snf5* C- $_{HtoA}$*-snf5* strains. D- Venn diagram of the genes upregulated during glucose-starvation.

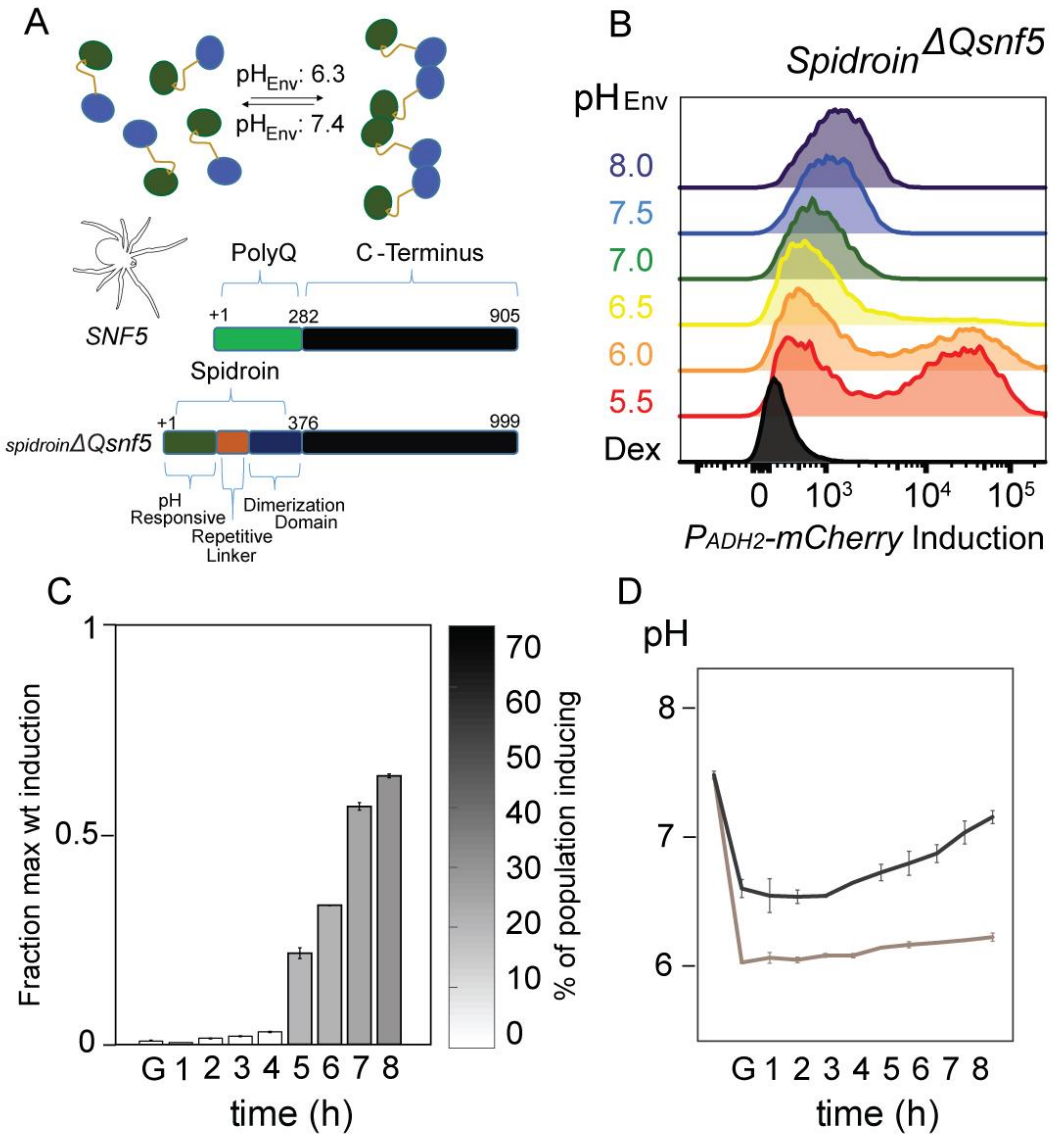


**Figure 6: A synthetic spidroin domain partially rescues pH-dependent induction of transcription.** A- Schematic representation of the aggregation behavior of spidroin. B- Induction of the *$P_{ADH2}$-mCherry* reporter with varying environmental pH: pH 5.5 (Red), pH 6.0 (Orange), pH 6.5 (Yellow), pH 7.0 (Green), pH 7.5 (Blue) and pH 8.0 (dark Blue). C- Quantification of reporter expression from (B) at various time points after glucose withdrawal. The Y axis is the intensity of fluorescent reporter (normalized to the levels of wild type control cells), shading corresponds to the percentage of cells inducing at each time point. D- Quantification of cytosolic pH from B.